phys. stat. sol. (b) **223**, 799 (2001)

Subject classification: 74.50.+r; 74.60.Ec; 74.62.–c; 74.80.Dm; S1.1

Synthetic Analyses of T_c and H_{c2} of NbTi/Nb Superconductor/Superconductor Superlattice

Y. OBI[1]) (a), M. IKEBE (b), H. FUJISHIRO (b), K. TAKANAKA (c), and H. FUJIMORI (a)

(a) Institute for Materials Research, Tohoku University, 2-1-1 Katahira, Aoba-ku, Sendai 980-8577, Japan

(b) Faculty of Engineering, Iwate University, 4-3-5 Ueda, Morioka 020-8551, Japan

(c) Faculty of Engineering, Tohoku University, Aramaki-aza-aoba, Aoba-ku, Sendai 980-8579, Japan

(Received March 21, 2000; in revised form August 16, 2000)

Based on an improved calculation formalism of the proximity effect, the transition temperature T_c, the parallel ($H_{c2\parallel}$) and perpendicular ($H_{c2\perp}$) critical fields of the $Nb_{50}Ti_{50}$/Nb superlattice have been analyzed as a function of the structural modulation wavelength λ_s. T_c, $H_{c2\parallel}$ and $H_{c2\perp}$ have been calculated using a unified set of the material parameters and allowing for the transition of the center of the order parameter between the NbTi and Nb layers. The calculation has systematically reproduced the characteristics of $H_{c2\parallel}$ and $H_{c2\perp}$ including the two-step dimensional crossover of $H_{c2\parallel}(T)$ and the anomalous upward curvature of $H_{c2\perp}(T)$.

1. Introduction

It is now well known that in superconductor/normal metal (S/N) superlattices, quasi-two-dimensional (q-2D) superconductivity is realized and the critical field parallel to the layer ($H_{c2\parallel}$) exhibits a dimensional crossover at T_D from three-dimension (3D) for $T > T_D$ to q-2D for $T < T_D$ [1–6]. Takahashi and Tachiki [7–9] predicted that, under appropriate conditions, superconductor/superconductor (S/S′) superlattices with different electron diffusion constants D exhibit a more complicated two-step dimensional crossover associated with a jump of the center position of the order parameter. With decreasing temperature T, the dimensionality of the superconductivity at first changes from 3D to q-2D at T'_D. In this q-2D state (2D′) the center of the order parameter is situated in the S′ layer with the larger D value. With the further decrease of T, the center of the order parameter shifts from the S′ layer to the S layer with the smaller D value at T^*_D and another q-2D state (2D*) is realized. Experimentally, the dimensional crossover appears most clearly as an inflection point in the parallel critical field $H_{c2\parallel}$ versus T curves [10–13].

In our previous papers [14, 15], we reported an anomalous depression of the superconducting transition temperature T_c of NbTi/Nb (S/S′) superlattices with decreasing structural modulation wavelength λ_s. The depression of T_c was attributed to the T_c drop of the Nb layer (T'_{cs}) with decreasing thickness and analyses were made for typical two cases. In the case (i) the T'_{cs} drop was attributed to the decrease in the electron density

[1]) Corresponding author; Fax: 81-22-215-2096; Tel.: 81-22-215-2097; e-mail: obi@imr.tohoku.ac.jp

of state N of the Nb layer and in the case (ii) it was attributed to the decrease of the BCS potential V of Nb. The calculations were performed based on an improved formalism of the proximity effect, which reproduced the experimental T_c versus λ_s dependence equally well for both cases and we could not conclude which model was more likely to correspond to the actual case.

In the present paper, we try to analyze $T_c(\lambda_s)$, $H_{c2\parallel}(T)$ and the perpendicular critical field $H_{c2\perp}(T)$ self-consistently based on the advanced formalism of the proximity effect [16–19] using a unified set of material parameters. $H_{c2\parallel}(T)$ of the present $Nb_{50}Ti_{50}/Nb$ superlattice with $\lambda_s = 120$ Å shows the characteristic two-step crossover. $H_{c2\perp}(T)$ shows a clear upward curvature for large λ_s values, which also seems to be peculiar to S/S′ superlattices with different D values [20, 21]. It is meaningful to examine if such peculiar behavior of the upper critical fields can be reproduced together with the λ_s dependence of T_c on a same footing.

2. Theoretical Background [18]

Takahashi and Tachiki [7] made an eigenfunction expansion for the de Gennes kernel and rewrote the equations to determine H_{c2} of the superconducting superlattices with spatial variations of the BCS interaction constant V, the density of states N and the diffusion constant D. They showed that 1. for the case with the spatial variation of D and V, one can obtain $H_{c2\parallel}$ taking into account only the lowest eigenstate and eigenfunction for the secular equation. 2. For the case with the spatial variation of N, it is necessary to take account of all the eigenvalues and eigenfunctions. For the case 2, Takahashi and Tachiki actually made an approximation to use only the lowest eigenstate, which is valid only for small values of N_s'/N_s. In the present calculations of $H_{c2\parallel}$ and $H_{c2\perp}$, the finite element method is applied to the equations derived on the basis of the Takahashi-Tachiki formalism. The finite element method permits us to take account of the higher eigenvalues and eigenfunctions besides the lowest ones. In the following, we describe an outline of the theoreticals used in the present calculation.

The eigenfunctions $\Psi_\lambda(\mathbf{r})$ to expand the de Gennes kernel satisfy the equation [7, 22]

$$-\hbar D(\mathbf{r}) \left(\nabla - \frac{2ie}{\hbar c} A(\mathbf{r}) \right)^2 \Psi_\lambda(\mathbf{r}) = E_\lambda \Psi_\lambda(\mathbf{r}) , \tag{1}$$

where $A(\mathbf{r})$ is the vector potential. The boundary conditions postulate that the quantities

$$\frac{\Psi_\lambda(\mathbf{r})}{\sqrt{N(\mathbf{r})}} \quad \text{and} \quad \sqrt{N(\mathbf{r})}\, D(\mathbf{r}) \left(\nabla - \frac{2ie}{\hbar c} A(\mathbf{r}) \right) \Psi_\lambda(\mathbf{r}) , \tag{2}$$

are continuous at the interfaces of the superlattice. We assume that the BCS potential $V(\mathbf{r})$, the density of states $N(\mathbf{r})$ and the diffusion constant $D(\mathbf{r})$ are constant inside each layer.

The order parameter $\Delta(\mathbf{r})$ and the pair function $F(\mathbf{r})$ are connected with $\Psi_\lambda(\mathbf{r})$ by the relation

$$\frac{\Delta(\mathbf{r})}{V(\mathbf{r})} = F(\mathbf{r}) = \sqrt{N(\mathbf{r})} \sum_\lambda C_\lambda \Psi_\lambda(\mathbf{r}) . \tag{3}$$

The pair function $F(\mathbf{r})$ then satisfies the same boundary conditions as $\sqrt{N(\mathbf{r})}\, \Psi(\mathbf{r})$ [22].

The transition temperature and the upper critical field of the superconducting superlattice are obtained by solving the following determinant raised from the de Gennes kernel for the coefficient c_λ [7, 17]:

$$\det \left| \delta_{\lambda\lambda'} - 2\pi k_B T \sum_{|\omega_n| \le \Omega_D} \frac{\langle \lambda | \, VN \, | \lambda' \rangle}{2\hbar \, |\omega_n| + E_\lambda} \right| = 0 \,, \tag{4}$$

where $\hbar\omega_n = (2n+1)\,\pi k_B T$, and Ω_D is the Debye frequency. For the ω_n summation in the above expression we take into account the effect of the Debye cutoff $\omega_n \le \Omega_D$, pointed out by Auvil and Ketterson [17] and approximate the sum as

$$I(E_\lambda) \equiv 2\pi k_B T \sum_{|\omega_n| \le \Omega_D} \frac{1}{2\hbar \, |\omega_n| + E_\lambda} = \log \left(\frac{2\hbar\Omega_D + E_\lambda}{4\pi k_B T} \right) - \Psi \left(\frac{1}{2} + \frac{E_\lambda}{4\pi k_B T} \right), \tag{5}$$

where we assume that the Debye cutoff frequency is same for both layers. By the use of Eqs. (4) and (5), T_c of superlattices in the small λ_s limit (the Cooper limit) is correctly reproduced. In the Werthamer [23] and the original Takahashi-Tachiki calculation [7], the small λ_s Cooper limit cannot be reproduced.

To have the eigenvalues and eigenfunctions of the lowest and the excite states, the following functional is considered:

$$\int d\nu \, N(\mathbf{r}) \left[\hbar D(\mathbf{r}) \left| \left(\nabla - \frac{2ie}{\hbar c} \, A(\mathbf{r}) \right) \phi_\lambda(\mathbf{r}) \right|^2 - E_\lambda \, |\phi_\lambda(\mathbf{r})|^2 \right]. \tag{6}$$

The variation of (6) with respect to $\phi_\lambda(\mathbf{r})$ gives an equation of the same form as Eq. (1),

$$-\hbar D(\mathbf{r}) \left(\nabla - \frac{2ie}{\hbar c} \, A(\mathbf{r}) \right)^2 \phi_\lambda(\mathbf{r}) = E_\lambda \phi_\lambda(\mathbf{r}) \,. \tag{7}$$

We impose the conditions on $\phi_\lambda(\mathbf{r})$ that

$$\phi_\lambda(\mathbf{r}), \quad \text{and} \quad N(\mathbf{r}) D(\mathbf{r}) \left(\nabla - \frac{2ie}{\hbar c} \, A(\mathbf{r}) \right) \phi_\lambda(\mathbf{r}) \,, \tag{8}$$

are continuous everywhere. The latter condition comes from the partial integral which appears at the interfaces by the variation of $\phi_\lambda(\mathbf{r})$. We relate the eigenfunction $\phi_\lambda(\mathbf{r})$ with $\Psi_\lambda(\mathbf{r})$ by the relation

$$\Psi_\lambda(\mathbf{r}) = \sqrt{N(\mathbf{r})} \, \phi_\lambda(\mathbf{r}) \,. \tag{9}$$

Then the finite element method can be applied to the functional (6). Numerical calculations in this study were performed on the computer program due to Takanaka.

3. Procedure of Experiments and Analyses

$Nb_{50}Ti_{50}$/Nb (S/S′) superlattice samples were fabricated by an rf sputtering method under symmetrical condition, i.e., $d_s = d'_s = \lambda_s/2$, λ_s being the structural modulation wavelength and d_s and d'_s the layer thicknesses of NbTi and Nb, respectively. The total thick-

Table 1
Parameters for the present calculation of T_c and H_{c2}

parameter	N'_s varied	fixed	V'_s varied
θ_D(K)	250[1])	250[1])	250[1])
T_{cs}(K)	8.4	8.4	8.4
T'_{cs}(K)	variable	8.1	variable
V_s (10^{-23} eV cm^3)	0.2684[2])	0.2684[2])	0.2684[2])
V'_s (10^{-23} eV cm^3)	0.34[3])	0.34[3])	variable
N_s (10^{23} states/eV cm^3)	1.0588[4])	1.0588[4])	1.0588[4])
N'_s (10^{23} states/eV cm^3)	variable	0.8273[5])	0.8470[5])
D_s (cm^2/sec)	1.36	1.36	1.36
D'_s (cm^2/sec)	variable	variable	variable
$\xi^s_{GL}(0)$(Å)	58.9	58.9	58.9
$H^s_{c2}(0)$(kOe)	85	85	85

[1]) Referred to Sasaki [24], $\theta_D = 250$ K is assumed for Nb and NbTi alloys as an average.
[2]) Determined from the relation $V_s = -[N_s \ln (T_{cs}/1.134\,\theta_D)]^{-1}$.
[3]) Referred to Gladstone et al. [25].
[4]) Deduced from the NbTi composition dependence of γ [24, 26–29] and the density of state of Nb [26–28, 30].
[5]) Determined from the relation $N'_s = -[V'_s \ln (T'_{cs}/1.134\,\theta_D)]^{-1}$ using $V'_s = 0.34$ and $T'_{cs} = 8.1$ for fixed case and $T'_{cs} = 8.8$ for varied case.
Non-marked: Experimental values. For T'_{cs} of fixed case, the value of thick film is used. D_s is determined from the relation $D_s = (4ck_B/\pi e)\,(\partial H_{c2\perp}(T)/\partial T)^{-1}|_{T=T_c}$ using $(\partial H_{c2\perp}(T)/\partial T)|_{T=T_c} = -8060$

ness of each superlattice was designed to be ~5000 Å. T_c, $H_{c2\parallel}$ and $H_{c2\perp}$ were determined by a four-terminal resistive method using a 10 T superconducting magnet. The small-angle X-ray diffraction patterns were taken to confirm the consistency between the designed λ_s and the actual one.

The calculations of $T_c(\lambda_s)$, $H_{c2\parallel}(T)$ and $H_{c2\perp}(T)$ were performed by an ACOS system computer at Tohoku University. For the calculations of T_c and $H_{cs\parallel,\perp}$, we need the values of several parameters of each layer, such as the GL coherence length at 0 K, $\xi^s_{GL}(0)$ of $Nb_{50}Ti_{50}$, the Debye temperatures θ^s_D and $\theta^{s'}_D$, the transition temperatures T_{cs} and T'_{cs}, the densities of states N_s and N'_s, the BCS potentials V_s and V'_s, and the ratio of the diffusion constant $\Delta D = D'_s/D_s$. The values of $\xi^s_{GL}(0)$ and T_{cs} were experimentally determined from the data of the sputtered $Nb_{50}Ti_{50}$ monolayer. θ^s_D and $\theta^{s'}_D$ were set to be 250 K and other values of the material parameters were taken from references. For the fitting of the experimental data, we chose the ratio of the diffusion constant, $\Delta D = D'_s/D_s$, and either N'_s or V'_s of the Nb layer as adjustable parameters. T'_{cs} was determined from the relation, $T'_{cs} = 1.134\,\theta^{s'}_D \exp(-1/N'V')$. The material parameters used for the fitting are summarized in Table 1.

4. Experimental Results

Figure 1a shows T_c data of $Nb_{50}Ti_{50}$/Nb superlattices as a function of the structural modulation wavelength λ_s, together with the results of the T_c calculations. In spite of almost the same T_c values ($\gtrsim$8 K) of both Nb and $Nb_{50}Ti_{50}$, $T_c(\lambda_s)$ of the superlattice substantially decreases with decreasing λ_s. If we calculate $T_c(\lambda_s)$ of the $Nb_{50}Ti_{50}$/Nb superlattice sticking to the standard set of the material parameters in Table 1 and keep-

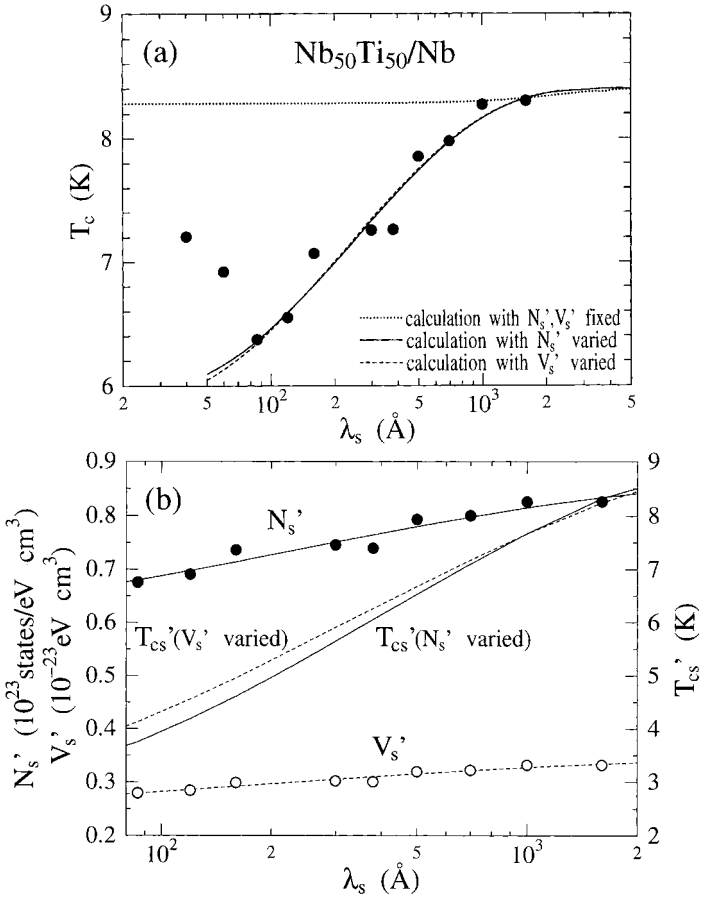

Fig. 1. a) T_c vs. λ_s of $Nb_{50}Ti_{50}$/Nb superlattices. The closed circles are experimental points. The dotted line almost independent of λ_s represents the fitting with a constant T'_{cs} (T_c of the Nb layer) value. The full line is the case (i) fitting changing the N'_s value as a fitting parameter with the ratio of the electron diffusion constant $\Delta D \equiv D'_s/D_s = 8$. The dashed line in the case (ii) fitting changing the V'_s value as a fitting parameter with $\Delta D = 9$ (see text). b) λ_s dependence of T'_{cs}, N'_s (for case (i)) and V'_s (for case (ii)) used in the present calculation. The full line is T'_{cs} vs. λ_s for the case (i) fitting and the dashed one for the case (ii) fitting

ing T_{cs} and T'_{cs} constant, the calculated $T_c(\lambda_s)$ curve derivates far higher from the observed one as shown by the dotted line in Fig. 1a. Then we must vary either T_{cs} or T'_{cs} as a λ_s dependent parameter to achieve the fitting. In a previous paper [15] we pointed out that T_c of the Nb layer (T'_{cs}) should decrease with decreasing λ_s.

Here we consider two typical cases of origin of the $T'_{cs}(\lambda_s)$ depression; a) N'_s varied case, which we denoted as case (i) and b) V'_s varied case, which we denoted as case (ii). The full line in Fig. 1a represents the calculated line for the case (i) and the dashed line represents that of case (ii). In order to keep consistency with the calculations of $H_{c2\parallel}$ and $H_{c2\perp}$ to be given later, the ratio of the diffusion constants ΔD ($= D'_s/D_s$) is set to be $\Delta D = 8$ for the case (i) and $\Delta D = 9$ for the case (ii). Both calculated curves reproduce well the experimental $T_c(\lambda_s)$ down to $\lambda_s = 86$ Å. For $\lambda_s = 60$, and 40 Å, however,

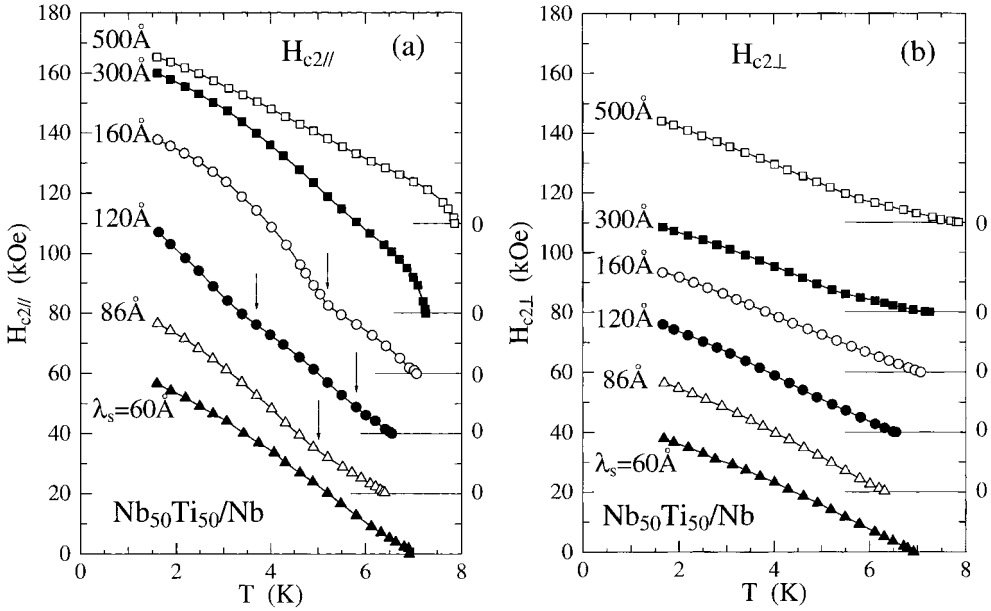

Fig. 2. Typical a) $H_{c2\parallel}$ and b) $H_{c2\perp}$ data as a function of T. The origin of the ordinate is shifted for each sample to get a clear view

T_c of NbTi/Nb again increases having a minimum around $\lambda_s \simeq 80$ Å. As we will mention later in connection with the $H_{c2\parallel}$ fitting, the non-neglectable alloying effect and/or interdiffusion of Nb and Ti atoms through the interface are considered to be the main origin of the T_c minimum. Figure 1b shows the λ_s dependences of T'_{cs} and N'_s (case (i)) and T'_{cs} and V'_s (case (ii)) necessary to achieve the T_c fitting given in Fig. 1a.

Figures 2a and 2b show the temperature dependences of $H_{c2\parallel}$ and $H_{c2\perp}$ of six typical NbTi/Nb samples. In both figures, the origins of the ordinates ($H_{c2} = 0$) are shifted to get clearer views. For $\lambda_s = 60$ Å in Fig. 2a, $H_{c2\parallel}$ shows the usual 3D behavior without any anomalous behavior. For $\lambda_s = 86$ Å, the crossover is seen in $H_{c2\parallel}(T)$ at $T \simeq 5.0$ K. For $\lambda_s = 120$ Å the two-step crossovers of $H_{c2\parallel}(T)$ occur at $T \simeq 5.8$ K and 3.7 K. For $\lambda_s = 160$ Å, the dimensional crossover from 3D to 2D is barely noticed in the very vicinity of T_c, followed by another clear crossover at $T \simeq 5.2$ K. For $\lambda_s = 300$ and 500 Å, $H_{c2\parallel}$ shows a 2D behavior following the relation $H_{c2\parallel} \propto (1-t)^{1/2}$, and no crossover phenomenon is observable.

In Fig. 2b, the temperature dependence of $H_{c2\perp}$ is not so drastically different from that of H_{c2} of usual 3D superconductors for $\lambda_s < 300$ Å. What is to be noticed in Fig. 2b is that a clear positive curvature anomaly (PCA) is noticed for $\lambda_s \geq 300$ Å. The existence of PCA in S/S′ multilayer systems with different D values of the sublayers was first predicted by Takahashi and Tachiki [7] in their pioneering paper.

5. Discussion

In order to perform systematic calculations of T_c, $H_{c2\parallel}$ and $H_{c2\perp}$, we must determine a self-consistent set of material parameters. For the H_{c2} fitting of S/S′ multilayers, the

ratio of the electron diffusion constants $\Delta D = D'_s/D_s$ is very important to decide the shape of the $H_{c2\|}(T)$ curves; the crossover temperature from 3D to 2D′ or from 2D′ to 2D* crucially depends on the ratio ΔD. Let us first discuss $H_{c2\|}(T)$ of $Nb_{50}Ti_{50}$/Nb with $\lambda_s = 120$ Å, which shows the typical two-step crossover. The results of the calculations using the material parameters of Table 1 and with ΔD as a variable parameter are shown in Figs. 3a and b. In Fig. 3a V'_s is kept the same as that of bulk Nb, while N'_s is varied to give the reduced T'_{cs} for $\lambda_s = 120$ Å. The calculation in Fig. 3a corresponds to the case (i) of the T_c calculation in Fig. 1b. In Fig. 3b, on the other hand, N'_s is kept the same as that of bulk Nb, while V'_s is varied to give the reduced T'_s which corresponds to the case (ii) in Fig. 1b. In these figures, the thick lines represent the calculated results with the center of the order parameters situated in the S layer (NbTi layer) and the thin lines represent those with the center of the order parameter situated in the S′ layer (Nb layer). According to the calculations for $\lambda_s = 120$ Å, the two-step crossover is expected for both case (i) and (ii) for $\Delta D \gtrsim 6$. In Figs. 3a and b, all thick and thin lines are almost indistinguishable between $T_c/T_{cs} \simeq 0.78$ and $T/T_{cs}(\equiv t') \simeq 0.7$. This fact means that the dimensionality of the superconductivity of $Nb_{50}Ti_{50}$/Nb with $\lambda_s = 120$ Å

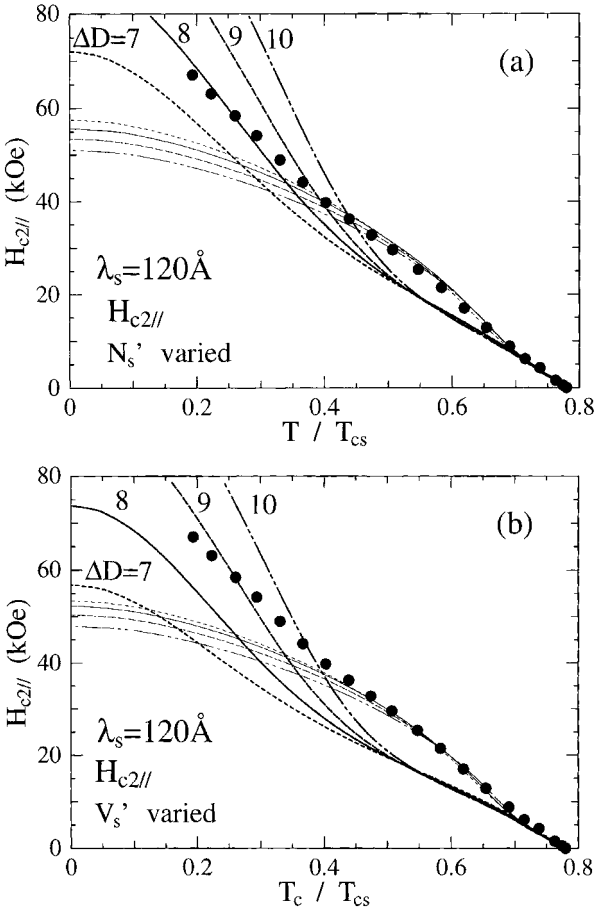

Fig. 3. a) Case (i) fitting for $H_{c2\|}$ of the $\lambda_s = 120$ Å sample. The N'_s value is set to be 0.6976×10^{23} states/eV cm^3 based on the result of N'_s-calculation (see Fig. 1b), while the bulk Nb value is used for the V'_s value ($= 0.34 \times 10^{-23}$ eV cm^3). The thick and thin lines represent the calculated results with the center of the order parameter in the NbTi(S) and Nb(S′) layer, respectively b) Case (ii) fitting for $H_{c2\|}$ of the $\lambda_s = 120$ Å sample. The V'_s is set to be 0.2858×10^{-23} eV cm^3 based on the result of V'_s-calculation (see Fig. 1b), while the bulk Nb value is used for the N'_s value ($= 0.8470 \times 10^{-23}$ states/eV cm^3). The thick and thin lines represent the calculated results with the center of the order parameter in the NbTi and Nb layer, respectively

is 3D above $T'_D/T_{cs} \simeq 0.7$ and changes to q-2D below T'_D. In this q-2D state below T'_D, the center of the order parameter is located in the S′ layer, which we denote as the 2D′ state. In Figs. 3a and b, we notice that T'_D is not so much sensitive to the ΔD value and is nearly independent of ΔD for $7 \leq \Delta D \leq 10$. With further decrease of temperature, the thick lines cross the thin lines at T^*_D and surpass the thin lines for $T \lesssim T^*_D$. This means that the center of the order parameter shifts to the S layer (NbTi layer) at T^*_D and the superconductivity of the superlattice enters into another q-2D state, which we denote as 2D* state. Experimentally, the transition from the 2D′ to 2D* state occurs at $T^*_D/T_{cs} \simeq 0.4$ for $\lambda_s = 120$ Å and the calculation line with $\Delta D = 8$ of the case (i) in Fig. 3a and that with $\Delta D = 9$ of the case (ii) in Fig. 3b are both consistent with the experimental results. Comparing the $\Delta D = 8$ line in the case (i) and $\Delta D = 9$ line in the case (ii), the case (i) lines give somewhat a better fitting with experimental data, especially in the lower temperature region ($t' < 0.3$).

Figure 4 shows the fitting of $H_{c2\|}(T)$ of NbTi/Nb for $\lambda_s = 160$, 300 and 500 Å. The results are presented for both case (i) and (ii) calculations. The same parameter values as $\lambda_s = 120$ Å were used except for the N'_s and V'_s values. The N'_s values for the case (i) and V'_s values for the case (ii) were set to be consistent with $N'_s(\lambda_s)$ and $V'_s(\lambda_s)$ lines in Fig. 1b, to reproduce the experimental T_c values for each modulation wavelength λ_s. For the $\lambda_s = 160$ Å sample, for which $H_{c2\|}$ shows apparently one crossover at $t' \simeq 0.65$, the calculation indicates that the observed crossover actually corresponds to T^*_D from 2D′ to 2D*, and T'_D exists just below T_c ($T'_D/T_{cs} \simeq 0.81$, $T_c/T_{cs} \simeq 0.84$). Though the calculation lines somewhat derivate downward from experimental $H_{c2\|}(T)$ near T_c and the calculated T^*_D/T_c ($\simeq 0.68$) is slightly higher than the experimental one, both fittings for the cases (i) and (ii) are satisfactorily equall as a whole.

The dimensionality of superconductivity is q-2D for $\lambda_s = 300$ and 500 Å and the $H_{c2\|}$ calculations suggest that the superconductivity of those samples is in the 2D* state over the whole temperature range

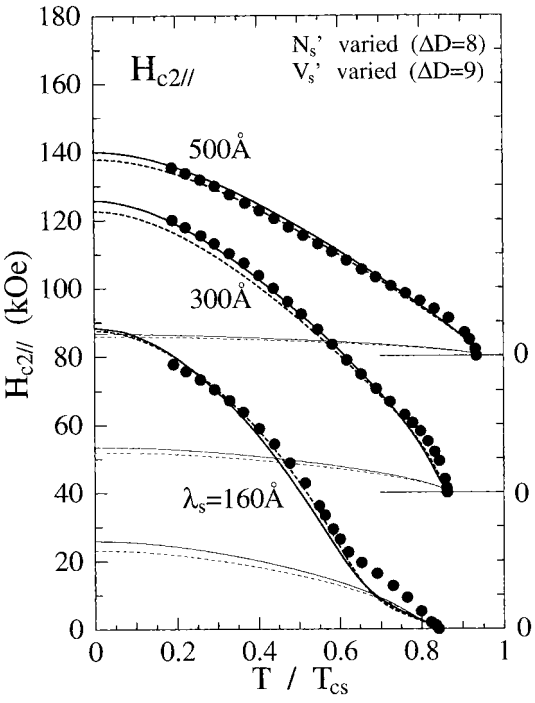

Fig. 4. $H_{c2\|}$ fitting for $\lambda_s = 160$, 300 and 500 Å samples. The full lines represent case (i) fitting, where N'_s is set to be 0.7140×10^{23} (160 Å), 0.7511×10^{23} (300 Å) and 0.7801×10^{23} (500 Å) states/eV cm^3 with $\Delta D = 8$. The dashed lines represent the case (ii) fitting, where V'_s is set to be 0.2918×10^{-23} (160 Å), 0.3050×10^{-23} (300 Å) and 0.3150×10^{-23} eV cm^3 (500 Å) with $\Delta D = 9$. The thick and thin lines are the calculated results with the center of the order parameter in the NbTi and Nb layer, respectively

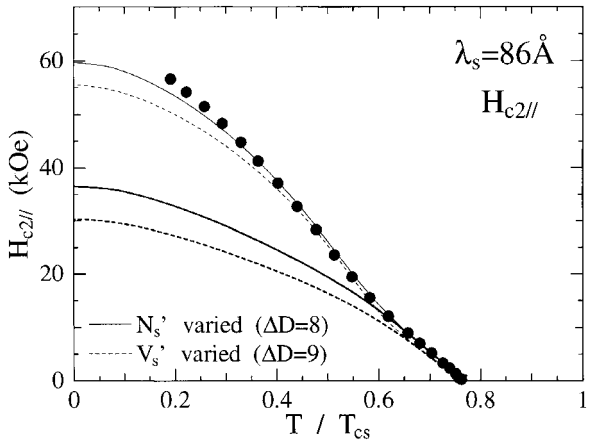

Fig. 5. $H_{c2\|}$ fitting for the $\lambda_s = 86$ Å sample. The full and dashed lines represent case (i) ($N'_s = 0.6800 \times 10^{23}$ states/eV cm^3; $\Delta D = 8$) and case (ii) ($V'_s = 0.2791 \times 10^{-23}$ eV cm^3, $\Delta D = 9$) fittings, respectively. The thick and thin lines represent the calculated $H_{c2\|}(T)$ with the center of the order parameter in the NbTi and Nb layer, respectively

below T_c with the center of the order parameter in the NbTi layer. Comparing the fitting lines for the cases (i) and (ii), the line of the case (i) is more satisfactorily for $\lambda_s = 300$ Å.

Figure 5 shows the $H_{c2\|}$ fitting results for the NbTi/Nb with $\lambda_s = 86$ Å. In this sample the one-step crossover occurs at around $t' \simeq 0.65$ and the calculation indicates that the crossover corresponds to T'_D from 3D to 2D′. With this small layer thickness ($d_{NbTi} = d_{Nb} = \lambda_s/2 = 43$ Å), the center of the order parameter is situated in the Nb layer below T'_D and does not shift to the NbTi layer down to 0 K. The present calculation assumes that $\xi^s_{GL}(0)$, the GL coherence length at 0 K, is 58.9 Å. The calculation suggests that $d_{NbTi} = 43$ Å is not thick enough to localize the order parameter in the NbTi layer to take full advantage of its smaller $\xi_{GL}(0)$ value. Comparing the lines for the cases (i) and (ii) in Fig. 5, we notice that the lines for the case (i) again result in a somewhat better fitting than for the case (ii).

Figure 6 shows the result of the case (i) fitting for $H_{c2\|}(T)$ of NbTi/Nb with $\lambda_s = 60$ Å. As we have mentioned already in Fig. 1a, T_c for this sample deviates upwards from the extrapolation of the calculated line and we suggest an interdiffusion

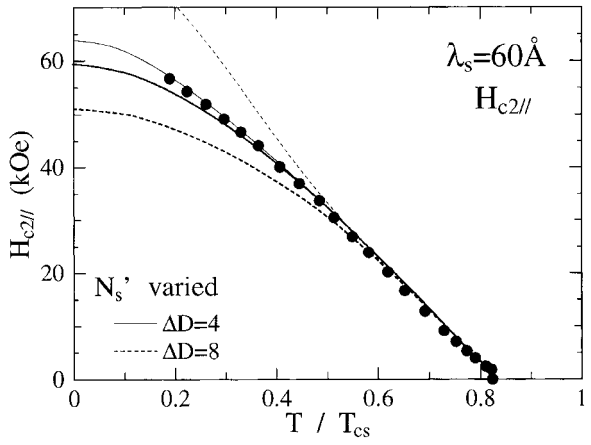

Fig. 6. Case (i) fitting for $H_{c2\|}$ of the $\lambda_s = 60$ Å sample. N'_s is set to be 0.7272×10^{23} states/eV cm^3 to give the observed T_c. The dashed lines represent the calculated results for $\Delta D = 8$ and the full ones those for $\Delta D = 4$. The thick and thin lines are the results with the center of the order parameter in the NbTi and Nb layer, respectively

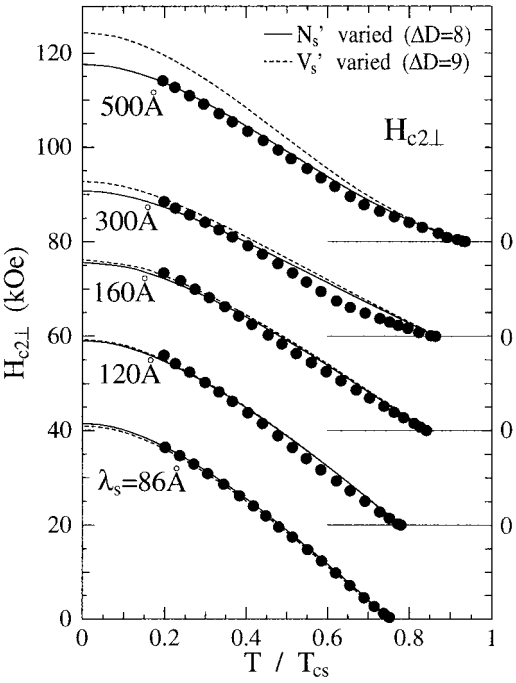

Fig. 7. $H_{c2\perp}$ fittings for the typical $Nb_{50}Ti_{50}$ superlattices. The full lines represent the case (i) fitting ($\Delta D = 8$) and the dashed lines show case (ii) fitting ($\Delta D = 9$)

through the interface as a possible origin [15]. In order to remedy the deviated T_c value, we adopted a higher value of N'_s ($=0.7272 \times 10^{23}$ states/eV cm^3) than that of Fig. 1b. If we stick to $\Delta D = 8$, however, the calculated lines do not reproduce the experimental data as shown in the figure. By scanning the ΔD values we found that $\Delta D = 4$ lines reproduce the experimental $H_{c2\parallel}(T)$. If the mixing of NbTi and Nb components through the interface becomes important, the diffusion constant D'_s of the Nb layer may become smaller due to the impurity scattering by immigrant Ti atoms. Thus, the smaller effective value of $\Delta D = D'_s/D_s$ may be consistent with the interdiffusion model for this small λ_s superlattice.

Finally, let us discuss the λ_s dependence of the perpendicular critical field $H_{c2\perp}(T)$ of NbTi/Nb superlattices. Figure 7 shows the fitting lines of $H_{c2\perp}(T)$ for $\lambda_s = 86$, 120, 160, 300 and 500 Å which were calculated using the same set of parameter values as for T_c and $H_{c2\parallel}(T)$ fittings. The overall agreement between the theoretical lines and the experimental data is satisfactory for the case (i) calculations. The case (ii) calculation lines with varying V'_s deviate from the experimental data for $\lambda_s = 300$ and 500 Å.

The $H_{c2\perp}$ versus t' lines in Fig. 7 show a clear positive curvature anomaly (PCA) for $\lambda_s = 300$ Å and 500 Å. As Takahashi and Tachiki [7] suggested for S/S′ superlattices with different D values of sublayers, the PCA anomaly occurs because the pair function for the order parameter, which are widely spread over several layers near T_c, become gradually localized in the S layers with smaller D as temperatures decrease. Our present $H_{c2\perp}(T)$ calculations well reproduce the upward curvature of $H_{c2\perp}$ for $\lambda_s = 500$ Å, though the calculation line for $\lambda_s = 300$ Å does not fully account for the observed very clear PCA anomaly.

6. Summary

The superconductor/superconductor (S/S′) superlattices, $Nb_{50}Ti_{50}$/Nb multilayers, were fabricated by a dual sputtering method over a wide range of structural modulation wavelenghths λ_s. The transition temperature T_c, the parallel critical field $H_{c2\parallel}(T)$ and the perpendicular critical field $H_{c2\perp}(T)$ were resistively measured. The experimental

results were synthetically analyzed based on an improved formalism of the proximity effect. From the anomalous depression of T_c of the superlattice, it was concluded that the T_c depression of the Nb sublayer with decreasing λ_s is responsible for the T_c depression of $Nb_{50}Ti_{50}$/Nb. The analyses of $H_{c2\parallel}(T)$ and $H_{c2\perp}(T)$ indicated that the degradation of T_c of the Nb sublayer should be mainly caused by the reduction in the elctron density of state N rather than by reduction of the BCS potential V. For $\lambda_s \geq 86$ Å, the calculated lines using a unified set of material parameter values minutely reproduced the behavior of $H_{c2\parallel}(T)$ and $H_{c2\perp}(T)$, including the two step crossover in $H_{c2\parallel}(T)$ characteristic of S/S′ superlattices. For $\lambda_s = 60$ Å, the $H_{c2\parallel}$ analyses provide an evidence of the interdiffusion effect as a reduction of the diffusivity ratio D'_s/D_s of the NbTi and Nb sublayers. The calculation also reproduced the anomalous upward curvature in $H_{c2\perp}(T)$ semi-quantitatively.

Acknowledgement The authors are grateful to the Center for Low Temperature Science of Tohoku University for the use of the 10 T superconducting magnet.

References

[1] C. S. L. Chun, G. G. Zheng, J. L. Vincent, and I. K. Schuller, Phys. Rev. B **29**, 4915 (1984).
[2] W. P. Lowe and T. H. Geballe, Phys. Rev. B **29**, 4961 (1984).
[3] K. Kanoda, H. Mazaki, N. Hosoito, and T. Shinjo, Phys. Rev. B **35**, 6736 (1987).
[4] B. Y. Jin and J. B. Ketterson, Adv. Phys. **38**, 189 (1989).
[5] J. W. P. Hsu, S. I. Park, G. Deutscher, and A. Kapitulnik, Phys. Rev. B **43**, 2648 (1991).
[6] Y. Obi, S. Takahashi, H. Fujimori, M. Ikebe, and H. Fujishiro, J. Low-Temp. Phys. **96**, 1 (1994).
[7] S. Takahashi and M. Tachiki, Phys. Rev. B **33**, 4620 (1986).
[8] S. Takahashi and M. Tachiki, Phys. Rev. B **34**, 3162 (1986).
[9] M. Tachiki and S. Takahashi, Physica C **153/155**, 1702 (1988).
[10] Y. Obi, M. Ikebe, Y. Muto, and H. Fujimori, Jpn. J. Appl. Phys. Suppl. **26**, 1445 (1987).
[11] M. G. Karkut, V. Matijasevic, L. Antognazza, J. M. Triscone, N. Missert, M. R. Beasley, and O. Fischer, Phys. Rev. Lett. **60**, 173 (1988).
[12] J. Aarts, K. J. de Korver, and P. M. Kes, Europhys. Lett. **12**, 447 (1990).
[13] Y. Kuwasawa, U. Hayano, T. Tosaka, S. Nakano, and S. Matuda, Physica C **165**, 173 (1990).
[14] Y. Obi, M. Ikebe, H. Fujishiro, and H. Fujimori, Physica C **235/240**, 2561 (1994).
[15] Y. Obi, M. Ikebe, and H. Fujimori, J. Phys. Soc. Jpn. **66**, 3600 (1997).
[16] P. R. Auvil and J. P. Ketterson, Jpn. J. Appl. Phys. **26**, 1461 (1987).
[17] P. R. Auvil and J. B. Ketterson, Solid State Commun. **67**, 1003 (1988).
[18] K. Takanaka, J. Phys. Soc. Jpn. **60**, 1070 (1991).
[19] A. Lodder and R. T. W. Koperdraak, Physica C **212**, 81 (1993).
[20] Y. Kuwasawa and T. Nojima, Czech. J. Phys. **46**, S2-745 (1996).
[21] Y. Kuwasawa, T. Nojima, S. Hwang, B. J. Yuan, and J. P. Whitehead, Physica B **222**, 92 (1996).
[22] P. de Gennes, Phys. Kondens. Mater. **3**, 225 (1964).
[23] N. R. Werthamer, Phys. Rev. **132**, 2240 (1963).
[24] T. Sasaki, Doctoral Thesis, Tohoku Univ., 1991.
[25] G. Gladstone, M. A. Jensen, and J. R. Schrierrer, Superconductivity, Vol. 2, Ed. R. D. Parks, Marcel Dekker, New York 1969 (p. 734).
[26] B. Y. Sukharevskii and A. V. Alapina, Soviet Phys. – JETP **27**, 897 (1968).
[27] B. Y. Sukharevskii, I. S. Shchetkin, and I. I. Falko, Soviet Phys. – JETP **33**, 152 (1971).
[28] E. M. Savitskii, V. V. Baron, Yu. V. Efimov, M. I. Bychkova, and L. F. Myzenkova, Superconducting Materials, Plenum Press, New York 1973.
[29] S. A. Elrod, J. R. Miller, and L. Dresrer, Adv. Cryog. Eng. **28**, 601 (1982).
[30] D. E. Eastman, Solid State Commun. **7**, 187 (1969).